

# Supplementary Material for “Global Dataset of Extreme Sea Levels and Coastal Flood Impacts over the 21st Century”

## S.1. Technical Validation

Global data of the type presented here, have a number of potential uncertainties. These uncertainties may be scenario based (e.g. greenhouse gas emission scenarios), epistemic (e.g. model based errors), and stochastic (e.g. natural variability of climatic systems) ( 1). All the global datasets used to create the database presented here are publicly available, except GTSR surge levels, (see “Methods”) and these datasets have been validated/quality controlled within their respective analyses (see “Description of the Datasets Used”).

Here, we address the potential uncertainty sources by validating the combined data against observed recordings of tide gauges, comparisons with previous studies, as well as through sensitivity analyses by employing different topography and *RSLR* datasets (see “Methods”).

### ***S.1.1. Validation of historical sea level timeseries (i.e. TSL) and ESL against Tide Gauge Recordings***

In the study of Kirezci et al ( 2) the historical timeseries (*TSL*) and calculated *ESL* were validated against the quasi-global GESLA-2 tide gauge dataset at 681 locations. The impact of the wave setup component (*WS* in “Methods” Eq.1) on the historical *TSL* and *ESL* was investigated extensively by Kirezci et al ( 2). This was undertaken using 3 methods: (i) applying two different *WS* evaluation approaches (i.e., SPM and Stockdon et al ( 3) methods), (ii) employing two global reanalysis datasets for offshore wave conditions (i.e., ERA-I and GOW-2), and (iii) investigating the bed slope sensitivity on *WS* (for bed slopes of 1/15, 1/30 and 1/100). Kirezci et al ( 2) concluded that it was appropriate to consider a mid-range bed slope of 1/30 with the SPM approach to determine globally representative values of *WS*. Moreover, the GOW2 wave model was preferred for the evaluation of *WS*, due to its higher resolution in coastal environments than other global models ( 4).

Kirezci et al ( 2) determined that the mean *RMSE* between modelled and observed historical *TSL* for the 681 tide gauge locations was 0.21 m, with individual values of *RMSE* at more than 75% of these locations being less than 0.2 m and at 93% of the locations less than 0.5 m. However, small values of *RMSE* may still be important at coastal locations with smaller mean tidal amplitudes, such as enclosed basins (e.g. Mediterranean, Baltic Sea). Relative *RMSE*, where the *RMSE* between the model and observed *TSL* was normalized by the mean tidal amplitude at GESLA-2 tide gauge locations, were found to be less than 20% at the majority of the locations (68%). As part of the present study the correlation coefficient, *c*, between the tide gauge recordings and the historical *TSL* data was also determined. At 78% of the tide gauge locations,  $c > 0.8$  (Fig S1a). We also investigate the Nash-Sutcliffe Efficiency coefficient (*NSE*) ( 5) which represents the agreement between the observed and simulated timeseries data (Fig S1b). Here, it is observed that more than half of the coastal locations (61%) show good agreement, ( $NSE > 0.8$ ). Both for the correlation coefficient and *NSE*, lower values are generally seen in closed or semi-closed basins (e.g. Mediterranean,

west coast of Japan), where modelling *TSL* can be challenging due to insufficient resolution of bathymetry and limitations in the global atmospheric reanalysis models ( 6).

To validate performance of the dataset for historical extreme conditions, Kirezci et al ( 2) investigated the bias of the upper percentile values of *TSL* both with and without the *WS* contribution. It was shown that the inclusion of the *WS* component to *ESL* decreases the higher percentile bias against the observed tide gauge records. Inclusion of *WS* reduced the upper percentile bias by 60% for the 99<sup>th</sup> percentile component.

The Kirezci et al ( 2) study tested 10 extreme value analysis (EVA) approaches – these include: Gumbel and Generalised Extreme Value distributions using Annual Maxima; and Generalized Pareto and Exponential Distributions using the Peaks over Threshold Method with four threshold values (98, 98.5, 99, 99.5 percentile). At each of the tide gauge locations, the best fitting distributions were determined by values of *RMSE* of the higher percentiles (80<sup>th</sup>) between the distributions and the fitted data. A GPD function fitted to POT data with a 98<sup>th</sup> percentile threshold was selected as the preferred method to estimate the return periods of the *ESL*. To compare the observed and model extreme projections, Kirezci et al ( 2) compared the 20-year return period (RP20) *ESL* determined from both observed and modelled *TSL*, at locations where the tide gauge recordings had a duration of at least 20 years (i.e. over the period 1979-2014, 355 locations out of 681). Kirezci et al ( 2, 7) concluded that the model *TSL* and *ESL* are in good agreement with recorded tide gauge data. This result is further strengthened by the expanded analysis in Figure S1.

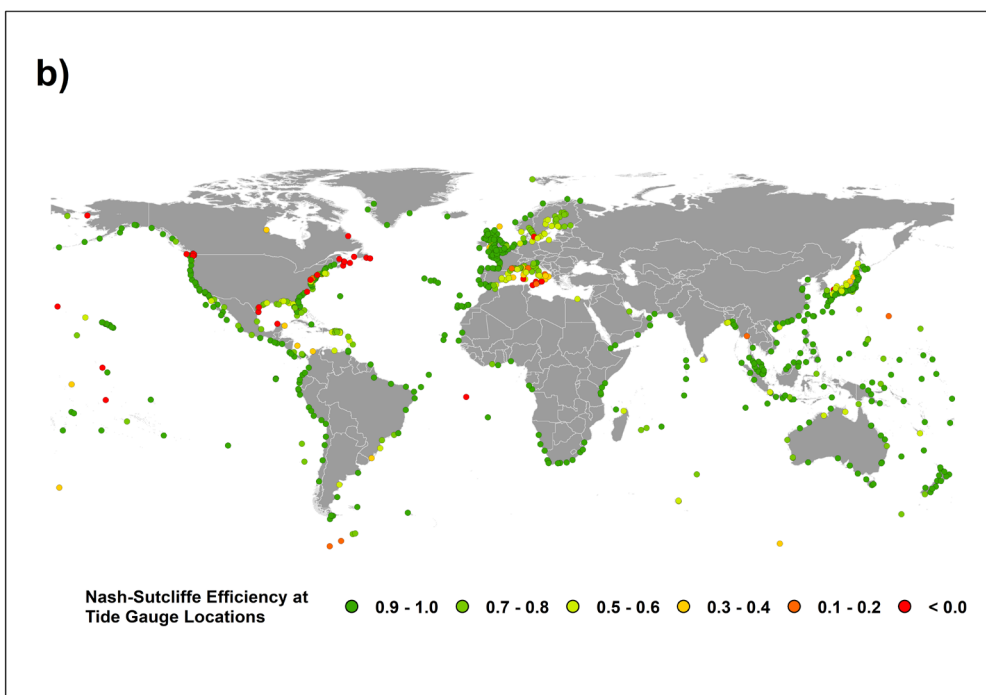
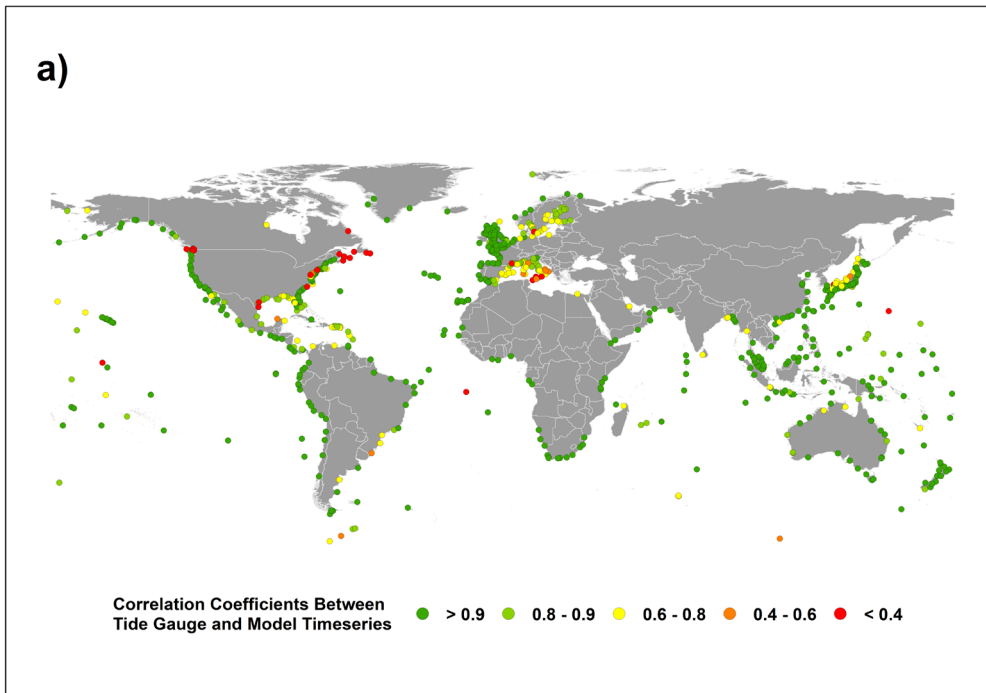


**Figure S1.** Global distributions of (a) Correlation Coefficient and (b) Nash-Sutcliffe Efficiency coefficient between tide gauge recordings and the historical *TSL* model data (Note the different colour scales). Figure constructed using ArcGIS v10.8.1.

### ***S.1.2. Comparison of the Inundation and Socioeconomic Impact Analyses with different DEM datasets***

The inundation extent is dependent on the digital elevation model (DEM) used to define the coastal topography. In order to test the sensitivity of the calculated inundation extent to the choice of DEM, additional analysis was undertaken using CoastalDEM ( 8) and results compared to the previously adopted MERIT DEM. As the spatial extent of the two DEMs differ, the common region of latitudes 60°N - 60°S was adopted for the comparison.

For the present-day case (2015), the global *EAPA* is 80M people/year and *EAD* is \$US758 B/year when CoastalDEM is used for the land elevation data, both results are two times larger than with the use of MERIT DEM. Under the no socioeconomic change scenario, *EAPA* is 112M people/year in 2050 and 254M people/year in 2100 for RCP85 for the CoastalDEM analysis. The *EAD* for the same adaptation scenario is \$US1.8 T/year in 2050 and \$US5.1 T/year in 2100 for RCP8.5. Both *EAPA* and *EAD* are again two times larger with Coastal DEM compared to results of the MERIT DEM analysis.

In 2100, with CoastalDEM, the *Adaptation Matching ESL Change case*, results in an *EAPA* increase up to 88M people/year and 204 M people/year for SSP1-2.6 and SSP3-8.5, respectively (Fig S2a). The *EAD* reaches up to \$US6.1 T/year and US\$10.4 T/year for SSP3-8.5 and SSP5-8.5, respectively (Fig S2b). These findings are in accordance with the smaller growth of global GDP under the SSP3 narrative, where the largest growth is estimated in the SSP5 narrative. When these values are compared with the MERIT analysis (Fig. S2; compare bar charts with lighter shades versus the darker shades), both *EAPA* and *EAD* outputs from CoastalDEM analysis are again approximately two times larger than the MERIT values.

The results using both DEMs for the cases of *Adaptation Matching ESL Change* and *No Additional Adaptation* are shown in Figure S2, again showing much larger values of *EAPA* and *EAD* when the CoastalDEM topographic data is used. Whilst the reliability of digital terrain models will undoubtedly improve in the future, at present, the choice of such models represents a major source of uncertainty in determining the socioeconomic implications of *ESL* change and *RSLR* ( 1).

The MERIT DEM was developed by correcting biases caused by multiple error sources such as speckle noise, stripe noise, absolute bias, and tree height bias from spaceborne DEMs that have been developed by utilising a number of satellite data sets and filtering techniques. CoastalDEM was developed using neural network trained data from the US and Australia and local LIDAR ground truth data.

Kirezci et al. ( 2, 7) adopted the MERIT DEM rather than CoastalDEM, as it has a longer history of application and was consistent with precedent in previous studies. Nevertheless, users should be aware that alternative choices of DEM can have significant impact on projected coastal impacts of flooding.

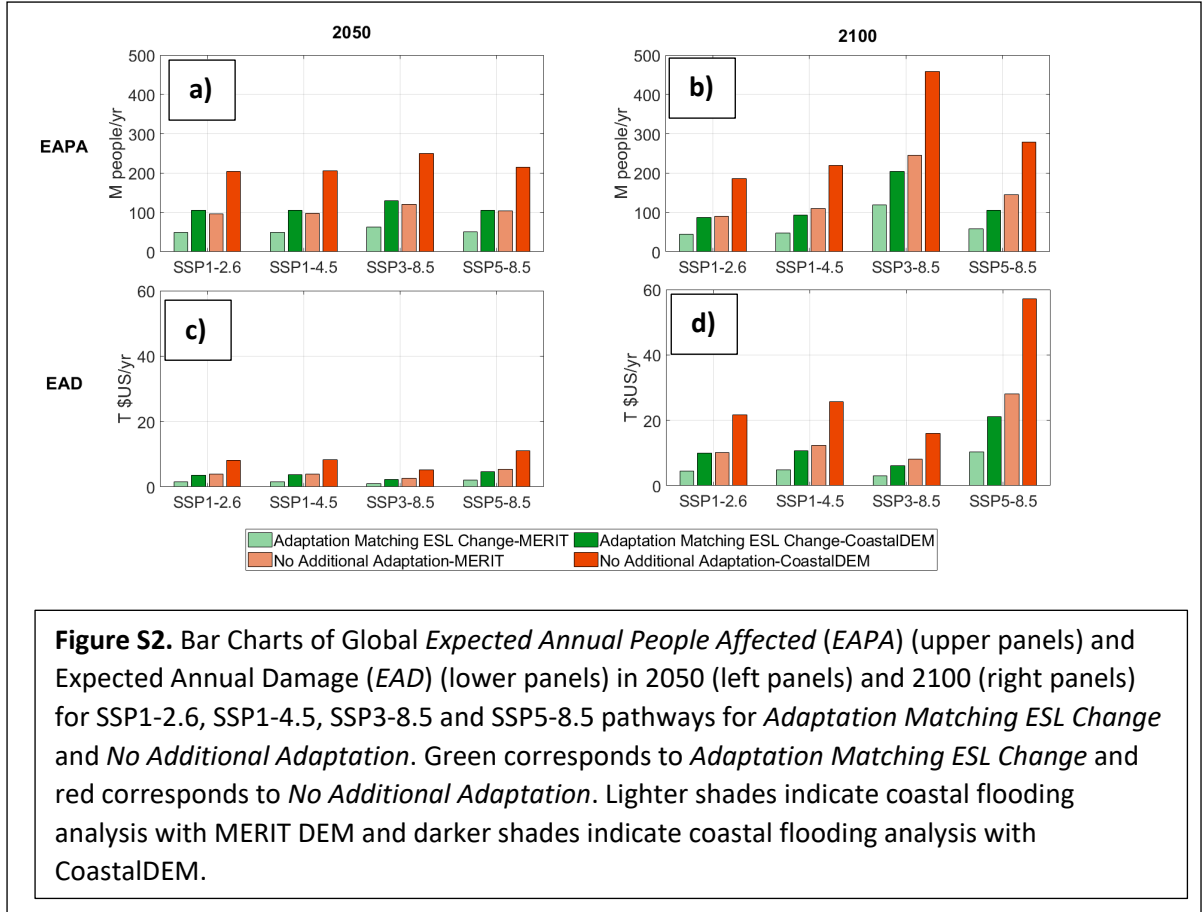


**Figure S2.** Bar Charts of Global *Expected Annual People Affected (EAPA)* (upper panels) and *Expected Annual Damage (EAD)* (lower panels) in 2050 (left panels) and 2100 (right panels) for SSP1-2.6, SSP1-4.5, SSP3-8.5 and SSP5-8.5 pathways for *Adaptation Matching ESL Change* and *No Additional Adaptation*. Green corresponds to *Adaptation Matching ESL Change* and red corresponds to *No Additional Adaptation*. Lighter shades indicate coastal flooding analysis with MERIT DEM and darker shades indicate coastal flooding analysis with CoastalDEM.

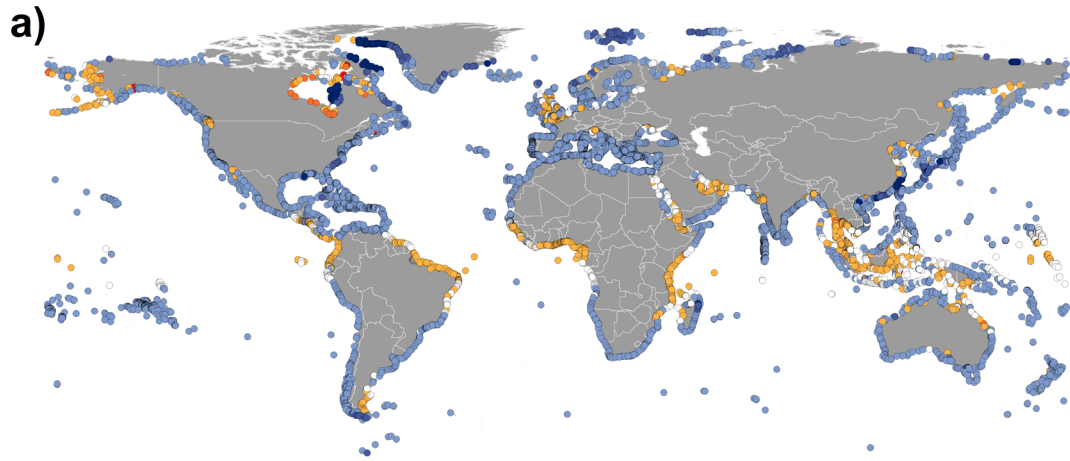
### S.1.3. Comparison with Previous Studies: ESL

It is a common approach when considering *ESL* to utilize the 100-year return period sea level ( $ESL_{100}^H$ ) for the present-day case. Below, global values of  $ESL_{100}^H$  from the present dataset are compared with three previous studies [Vousdoukas et al ( 9), Muis et al ( 10) and Vitousek et al ( 11)].

Vousdoukas et al ( 9) calculated global values of  $ESL_{100}^H$  by defining probability distribution functions (pdfs) of reanalysis tide, surge and wave setup, for the present-day and future periods. The pdfs were then combined using a Monte Carlo approach to extrapolate to higher return periods of *ESL*. Projected future changes in storm surge and wave conditions are also considered in the Vousdoukas et al ( 9) study. Figure S3a compares the difference between the present data set and that of Vousdoukas et al ( 9) for  $ESL_{100}^H$ . The Vousdoukas et al. ( 9) values are generally larger (negative difference in Fig. S3a) for most global coastlines, with the exception of the tropical and sub-tropical latitudes, Alaskan coastlines and Hudson Bay.

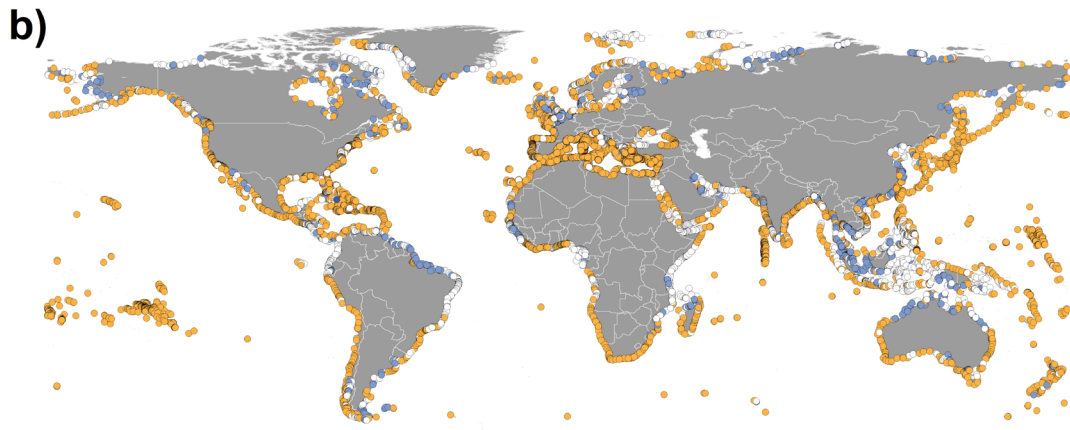
Muis et al ( 10) determined  $ESL_{100}^H$  using a similar approach to that adopted for the present dataset. The *TSL* contributors were added linearly (as in “Methods”, Eq.1), however, the *WS* component of the *TSL* was not considered (i.e.,  $TSL=T+S$ ). To determine the 100-year return period values, Muis et al ( 10) fitted a Gumbel distribution to Annual Maxima over 36-year *TSL* records. Figure S3b shows differences between the present dataset and that of Muis et al ( 10) for  $ESL_{100}^H$ . At most locations, the estimates of Muis et al. ( 10) are smaller, with the median difference being +0.15m with a standard deviation of 0.25m).

Vitousek et al ( 11) linearly combined reanalysis datasets, as in Eq. 1 (i.e. including  $WS$ ). To determine  $ESL^{H_{100}}$  they fitted a Generalized Extreme Value (GEV) distribution to the 3-largest annual maxima over 21-year time series. As shown in Fig. S3c, the values of Vitousek et al ( 11)  $ESL^{H_{100}}$  are slightly smaller than the present dataset at most coastal locations (median difference of +0.06 m with a standard deviation of 0.56m). It should be noted that the Vitousek et al ( 11) dataset does not include closed basins (e.g., Mediterranean, Hudson Bay, Black Sea). As a result, the number of data points compared, is only 68% of the total data from the present dataset.



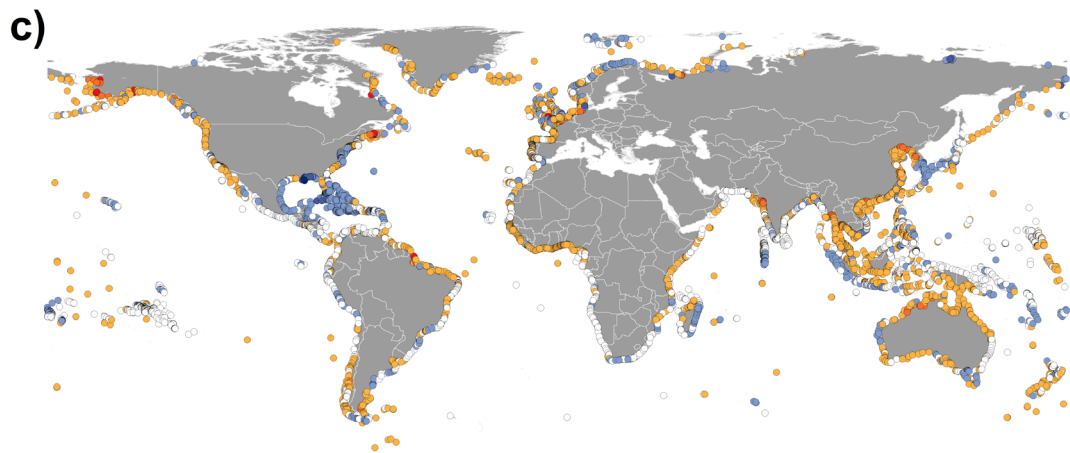
Differences of  $ESL^{H100}$  - Kirezci et al (2022) - Vousdoukas et al (2018) (m)

● < -2.5 ● (-2.5) - (-1.5) ● (-1.5) - (-0.1) ○ (-0.1) - (0.1) ● 0.1 - 1.5 ● 1.5 - 2.5 ● 2.5 <



Differences of  $ESL^{H100}$  - Kirezci et al (2022) - Muis et al (2016) (m)

● < -2.5 ● (-2.5) - (-1.5) ● (-1.5) - (-0.1) ○ (-0.1) - (0.1) ● 0.1 - 1.5 ● 1.5 - 2.5 ● 2.5 <



Differences of  $ESL^{H100}$  - Kirezci et al (2022) - Vitousek et al (2017) (m)

● < -2.5 ● (-2.5) - (-1.5) ● (-1.5) - (-0.1) ○ (-0.1) - (0.1) ● 0.1 - 1.5 ● 1.5 - 2.5 ● 2.5 <

**Figure S3.** Global distributions of the differences between the present case  $ESL^{H100}$  dataset and the results of (a) Vousdoukas et al ( 16), (b) Muis et al ( 10) and (c) Vitousek et al ( 11). Figure constructed using ArcGIS v10.8.1.

### **S.1.4. Comparison against Previous Studies: EAPA and EAD**

Due to the many potential adaptation scenarios which can be adopted to respond to projected future coastal flooding, comparisons for *EAPA* and *EAD* have been limited to the case of *No Additional Adaptation* (i.e. current defences are maintained but not upgraded and no new defences are constructed, but population and GDP change). Kirezci et al ( 7) showed that projections of *EAPA* and *EAD* for the present dataset (*No Additional Adaptation* case) fall between the values projected by Hinkel et al ( 12), Tiggeloven et al ( 13) and Schinko et al ( 14). Additionally, we have here also compared the present dataset with the study of Jevrejeva et al ( 15), which estimated the global annual damage costs (*EAD*) without additional adaptation and under global sea level rise with 1.5 °C (0.52 m) and 2 °C (0.63 m) temperature increases. For the case where the 2 °C target is not achieved, Jevrejeva et al ( 15) further considered global sea level rise under RCP 8.5 (0.86 m - median and 1.8 m - 95<sup>th</sup> percentile). For the impact modelling, Jevrejeva et al ( 15) used SSP2 for socioeconomic development by 2100. Jevrejeva et al ( 15) projected that, without future adaptation, the global *EAD* could be \$US10.2 T/year under a 1.5 °C temperature rise induced global sea level rise, and \$US14-\$27 T/year under an RCP8.5 scenario (beyond 2 °C temperature rise). This can be compared with SSP3-8.5 and SSP5-8.5 in the present dataset, where the data indicates - \$US 7.9T and \$US 39.0 T/year (95<sup>th</sup> percentile of SSP5-85, under *No Additional Adaptation* scenario), respectively. Again, the present dataset is reasonably consistent with the Jevrejeva et al ( 15) study.

## **References**

1. Hinkel, J. *et al.*, Uncertainty and bias in global to regional scale assessments of current and future coastal flood risk. *Earth's Future* ( e2020EF001882), 1-28 (2021).
2. Kirezci, E. *et al.*, Projections of global-scale extreme sea levels and resulting episodic coastal flooding over the 21st Century. *Scientific Reports* **10** (11629) (2020).
3. Stockdon, H. F., Holman, R. A., Howd, P. A. & Sallenger, A. H., Empirical parameterization of setup, swash, and runup. *Coastal Eng.* **53**, 573–588 (2006).
4. Perez, J., Menendez, M. & Losada, I. J., GOW2: A global wave hindcast for coastal applications. *Coastal Eng.* **124**, 43405 (2017).
5. Nash, J. E. & Sutcliffe, J. V., River flow forecasting through conceptual models Part 1 - A discussion of principles. *J. Hydrol.* **10**, 282-290 (1970).
6. Wolff, C. *et al.*, A Mediterranean coastal database for assessing the impacts of sea-level rise and associated hazards. *Scientific Data*, 180044 (2018).
7. Kirezci, E., Young, I. R., Ranasinghe, R., Lincke, D. & Hinkel, J., Global-scale analysis of socioeconomic impacts of coastal flooding over the 21st century. *Frontiers Mar. Sci.* **9**, 1024111 (2023).
8. Kulp, S. A. & S. B. H., New elevation data triple estimates of global vulnerability to sea-level rise and coastal flooding. *Nature Communications* **10** (4844) (2019).

9. Vousdoukas, M. I. *et al.*, Global probabilistic projections of extreme sea levels show intensification of coastal flood hazard. *Nature Communications* **9**, 2360 (2018).
10. Muis, S., Verlaan, M., Winsemius, H. C., Aerts, J. C. & Ward, P. J., A global reanalysis of storm surges and extreme sea levels. *Nat. Commun.* **7**, 11969 (2016).
11. Vitousek, S. *et al.*, Doubling of coastal flooding frequency within decades due to sea-level rise. *Scientific Reports* **1399**, 1-9 (2017).
12. Hinkel, J. *et al.*, Coastal flood damage and adaptation costs under 21st century sea-level rise. *Proc., Nat. Acad. Sci* **111**, 3292–3297 (2014).
13. Tiggeloven, T. *et al.*, Global-scale benefit–cost analysis of coastal flood adaptation to different flood risk drivers using structural measures. *Nat. Hazards Earth Syst. Sci.* (20), 1025–1044 (2020).
14. Schinko, T. *et al.*, Economy-wide effects of coastal flooding due to sea level rise: a multi-model simultaneous treatment of mitigation, adaptation, and residual impacts. *Environmental Research Communications* **2** (1) (2020).
15. Jevrejeva, S., Jackson, L. P., Grinsted, A., Lincke, D. & Marzeion, B., Flood damage costs under the sea level rise with warming of 1.5 °C and 2 °C. *Environmental Research Letters* (2018).
16. Vousdoukas, M. I. *et al.*, Climatic and socioeconomic controls of future coastal flood risk in Europe. *Nature Climate Change*, 776-780 (2018).
17. Oppenheimer, M. *et al.*, Sea Level Rise and Implications for Low-Lying Islands, Coasts and Communities. *IPCC Special Report on the Ocean and Cryosphere in a Changing Climate [H.-O. Pörtner, D.C. Roberts, V. Masson-Delmotte, P. Zhai, M. Tignor, E. Poloczanska, K. Mintenbeck, A. Alegría, M. Nicolai, A. Okem, J. Petzold, B. Rama, N.M. Weyer (eds.)]* (In press), 321-445 (2019).
18. Ericson, J. P., Vorosmarty, C. J., Dingman, S. L., Ward, L. G. & Meybeck, M., Effective sea-level rise and deltas: Causes of change and human dimension implications. *Global and Planetary Change* **50**, 63-82 (2006).
19. Syvitski, J. P. M. e. a., Sinking deltas due to human activities. *Nature Geoscience* **2**, 681–686 (2009).
20. Vafeidis, A. T. *et al.*, Water-level attenuation in global-scale assessments of exposure to coastal flooding: a sensitivity analysis. *Nat. Hazards Earth Syst. Sci.* **19**, 973–984 (2019).
21. Vousdoukas, M. *et al.*, Developments in large-scale coastal flood hazard mapping. *Natural Hazards and Earth System Sciences* **16** (8), 1841-1853 (2016).